OPEN

Flux Exclusion Superconducting Quantum Metamaterial: Towards Quantum-level Switching

V. Savinov[1], A. Tsiatmas[1], A. R. Buckingham[2], V. A. Fedotov[1], P. A. J. de Groot[2] & N. I. Zheludev[1]

[1]Optoelectronics Research Centre & Centre for Photonic Metamaterials, University of Southampton, SO17 1BJ, UK, [2]School of Physics and Astronomy & Centre for Photonic Metamaterials, University of Southampton, SO17 1BJ, UK.

Nonlinear and switchable metamaterials achieved by artificial structuring on the subwavelength scale have become a central topic in photonics research. Switching with only a few quanta of excitation per metamolecule, metamaterial's elementary building block, is the ultimate goal, achieving which will open new opportunities for energy efficient signal handling and quantum information processing. Recently, arrays of Josephson junction devices have been proposed as a possible solution. However, they require extremely high levels of nanofabrication. Here we introduce a new quantum superconducting metamaterial which exploits the magnetic flux quantization for switching. It does not contain Josephson junctions, making it simple to fabricate and scale into large arrays. The metamaterial was manufactured from a high-temperature superconductor and characterized in the low intensity regime, providing the first observation of the quantum phenomenon of flux exclusion affecting the far-field electromagnetic properties of the metamaterial.

S uperconducting electromagnetic metamaterials are attracting increasing attention due to low ohmic losses, high sensitivity to temperature and magnetic fields, as well as due to the exotic properties of the macroscopic quantum state of superconducting carriers[1], and essentially plasmonic nature of the electromagnetic response of superconductors[2,3]. Extraordinary transmission of superconducting hole arrays[4,5] and EIT-like behavior of a superconducting meta-molecule[6,7] have been observed. Moreover, temperature[8–12], magnetic field[13] and current control[14] of electromagnetic response of superconducting metamaterials have been demonstrated recently. Several groups have analyzed superconducting metamaterials with meta-atoms containing Josephson junctions[15–19], experiments have been conducted on single superconducting qubit meta-atoms[20,21] and one-dimensional Josephson junction metamaterials[22]. The recently discovered class of iron-based superconductors[23] promises to extend the superconductivity range even further into the terahertz spectrum. The combination of low losses and strong non-linearities over the broad spectral range thus makes the superconducting metamaterials a central topic in the sub-optical metamaterial research.

Here we introduce a new type of superconducting metamaterial that we brand as the flux exclusion quantum metamaterial. It exploits magnetic flux quantization as a source of its switching functionality but does not require Josephson junctions in its construction, making it much simpler to fabricate and scale into large arrays. The metamaterial was manufactured from a high-T_c superconductor film and its electromagnetic properties were characterized in the low intensity regime at cryogenic temperatures. In this metamaterial we observed large changes in the electromagnetic response due to the quantum phenomenon of flux exclusion. We also manufactured and characterized two other types of metamaterial arrays, the electromagnetic properties of which model the low and high magnetic flux states of the new quantum metamaterial, thus illustrating its potential for switching performance.

Results

Basic design and modeling. The coherent nature of the macroscopic quantum state of carriers in a superconductor dictates that the magnetic flux through a closed superconducting loop will be an integer multiple of the flux quantum $\Phi_0 \equiv h/2e \approx 2.1 \times 10^{-15}$ Wb, where h is the Plank's constant and e is the charge of the electron[24]. One may therefore deduce that in a much simplified picture, when resistive losses and kinetic inductance of the Cooper pairs are neglected, the response of the closed superconducting loop to ramped magnetic field (B_a) will be similar to that sketched in Fig. 1. At low magnitudes of the applied field the amplitude of the total magnetic flux
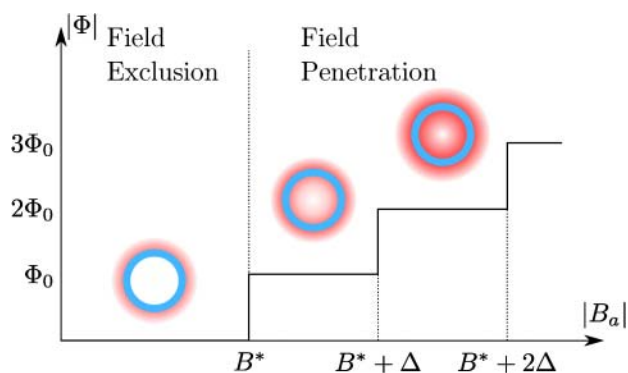
1

Figure 1 | The Flux Exclusion in Superconducting Ring. Idealized response of the closed superconducting loop to an applied magnetic field of amplitude $|B_a|$. At low amplitudes of the applied field, the amplitude of the total flux through the loop $|\Phi|$ stays close to zero. When the amplitude of the applied field increases to a critical value B^*, the amplitude of magnetic flux through the loop jumps to one flux quantum Φ_0. Further jumps occur every time the amplitude of the applied magnetic field increases by Δ. The insets are artistic impressions of the magnetic field configuration (red) around the superconducting loop (blue).

through the ring ($|\Phi|$) will be close to zero. As the amplitude of the applied field increases past a critical value B^*, the flux through the ring will increase to a flux quantum. After that the amplitude of the flux through the loop will grow in jumps, increasing by Φ_0 as the amplitude of the applied field is increased. One can distinguish two regimes: when the flux through the loop is zero despite the applied magnetic field and the regime when flux through the loop is greater than zero. We will refer to these two cases as field exclusion and field penetration regimes. The critical value of the applied field separating these two regimes will be discussed below.

At high frequencies the only way for the magnetic field to penetrate the closed superconducting loop is through local supression of the superconducting phase (at lower frequencies, for type-II superconductors, magnetic field can slip into the loop in form of Abrikosov vortices, but the vortex propagation velocities are too low[25,26] to penetrate through the width of realistic superconducting wire during a single high-frequency cycle in the Gigahertz range of frequencies). This is a fast process limited by the nonequilibrium electron-phonon interaction time, which is about 1 ps in high-T_c superconductors[27,28]. The superconducting state will be destroyed when the current in the closed loop reaches a critical value I_c. It follows, that when the applied magnetic field reaches $B^* = LI_c/S$, where L is the inductance of the closed loop and S is the area encircled by the loop, the superconductivity in the wire will be supressed and the first magnetic flux quantum will enter the loop. After the penetration by the first quantum, the remaining field to be screened will be $B^* - \Delta$, where $\Delta = \Phi_0/S$. The screening current will therefore be $I = I_c - \Phi_0/L$ i.e. lower than critical current and superconductivity in the loop will be restored. Following the first jump, there will be a new jump, in flux through the loop, every time the strength of the applied field reaches $B^* + m\Delta$, where m is a positive integer (see Pedersen[29] et al. for an experimental demonstration of this behaviour in the lower frequency range). Clearly the most interesting behavior will be observed for the loops where $B^* \approx \Delta$ (or $LI_c \approx \Phi_0$).

Here we suggest that this flux quantization mechanism may be engaged as a source of nonlinearity in the metamaterial. For this purpose, in the simplest implementation, we enclose the superconducting wire loop into a resonant split-ring resonator thus creating a meta-molecule. This meta-molecule will be a building block of the two-dimensional flat metamaterial array. We will call this design the flux exclusion quantum metamaterial. For normal radiation incidence on the array of such meta-molecules, the magnetic field

of the incident wave does not penetrate the array and therefore is not directly engaged in the flux quantization. However, an incident electromagnetic wave polarized along the split-ring resonator gap will drive an oscillating current in the resonator that will produce oscillating magnetic field embraced by the split ring. The superconducting wire loop inside the split-ring will respond depending on the amplitude of the generated magnetic field and therefore depending on the incident wave intensity: or it will block the field penetration at low levels of magnetic flux, or it will allow penetration at high levels, thus ensuring the nonlinear nature of the response. As a result, in the flux penetration regime, the closed loop will be continuously driven by the oscillating magnetic field from one flux state to the next one, up and down the ladder (Fig. 1), in much the same way as superconducting loops driven by the slowly varying external magnetic field previously shown by Silver & Zimmerman[30].

We shall note that electromagnetic functionality of the flux exclusion quantum metamaterial described here is distinctively different from the artificial atoms based on Josephson junctions, where the transition between the quantum energy levels of the meta-atom is achieved by absorption of single energy quanta of the incident wave[20,21]. In our case the resonant properties of the metamaterial are derived from the outer split-ring resonator of the meta-molecule which, at high frequency, acts as an LC circuit. Nonlinearity here is a result of inductance being a function of intensity: higher intensity levels of incident waves creates a larger magnetic flux through the ring. At a certain level of excitation the applied flux can drive transitions between the different quantum flux states of the inner ring, thus dynamically modifying the inductance and the resonant properties of the LC circuit (meta-molecule).

We illustrated the switching in the flux quantization metamaterial by modeling its response using two different metamaterial structures. One of them modelled the flux penetration regime. It was an array of split ring resonators without the superconducting wire loop inside. Another metamaterial modelled the flux exclusion regime. It was also an array of split ring resonators, but in addition, each resonator embraced a superconducting disk blocking the flux penetration through its center. We assumed in our modeling that the metamaterial structures were manufactured from thin films of high-temperature superconductor yttrium-barium-copper-oxide (YBCO). The full 3-dimensional Maxwell calculation of metamaterial transmission, using the two-fluid model of superconductivity of YBCO[31], illustrates the switching (see Fig. 2). Blocking the flux penetration through the area embraced by the split ring results in a 2.7 GHz shift of the transmission resonance. Such a shift would correspond to switching from the flux penetration state to the flux exclusion state in the flux quantization metamaterial with meta-molecules consisting of a superconducting rings embraced by split rings. Figure 2 also shows the redistribution of the magnetic field in the meta-molecule that arises due to switching.

To observe the switching, the incident field shall drive the flux quantization metamaterial to such a level that applied flux through the disk exceeds Φ_0. Simultaneously, the electrical current density in the outer perimeter of the disk shall reach the critical value that destroys superconductivity thus allowing the magnetic field to penetrate inside. From the models in Fig. 2 we estimated that, at resonance, the amplitude of the flux applied to the nested disks in the metamaterial (at temperature T = 77 K) would reach a few Φ_0 for the incident radiation intensity levels below $\sim$ 50 μW/cm^2. At such intensity the current density in the outer perimeter of the disk will be of the order of 10^4 A/cm^2. This is much smaller than the critical current density of the wire, which is approximately[32] 10^6 A/cm^2 at T = 77 K.

Woodcut metamaterial design. To approach the regime where flux quantization will be observable ($LI_c \approx \Phi_0$) one could operate the metamaterial very close to superconductor's critical temperature,
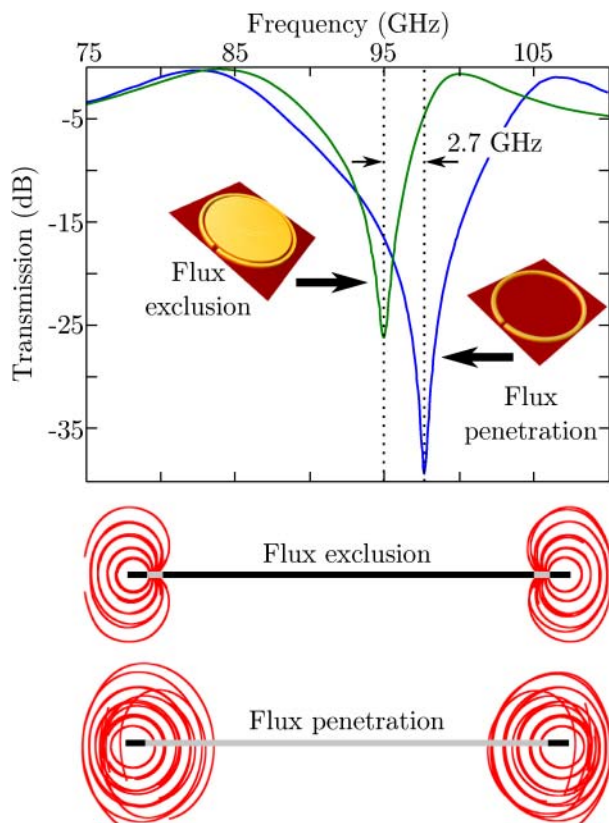
Figure 2 | **Switching in Flux Exclusion Superconducting Quantum Metamaterial.** Resonant curves correspond to two limiting regimes, the flux exclusion regime (low intensity, green curve) and flux penetration regime (high intensity, blue curve). The insets show the diagrams of the corresponding reference metamaterials (mimicking the corresponding limiting regimes). Both are modeled as a thin YBCO film on 1 mm-thick sapphire substrate. The unit cell sizes are 240 μm×240 μm. Outer and inner radii of the split ring resonators are 100 μm and 92 μm, respectively. The radius of the nested disk is 89 μm. The size of the gap in the split-ring is 8 μm. The metamaterials are driven by the normally-incident radiation with electric field polarized along the gap in the split-ring resonators. The insets below the main plot show the side view of the distribution of magnetic field in the two meta-molecules at their resonance.

thus lowering the critical current density. However, increasing the temperature leads to suppressed switching as Joule losses dampen the resonance. The high-frequency conductivity of high-T_c superconductors only changes within an order of magnitude as temperature approaches the critical value[33–35], but this moderate change has a profound effect on the resonant response of metamaterials[9,11,12]. To get around this problem we designed and manufactured a flux exclusion quantum metamaterial that is more complex than just a pattern of rings enclosed by the split rings that we used above to explain the principle of operation. Here, instead of enclosing a single superconducting ring, every split ring of the design embraces a cluster of smaller superconducting loops, resembling a wood cut, Fig. 3. In this design switching will be achieved simultaneously in a number of small loops. As the loops become smaller the same applied magnetic flux induces larger screening currents in them. Making the loops very small thus allows the screening currents to reach the critical value necessary for the suppression of superconductivity at the level of applied flux close to Φ_0. A variation of the sizes of enclosed superconducting loops also helps to achieve cascade switching at different excitation levels. We call this design a woodcut metamaterial.

We manufactured the woodcut metamaterial according to the design shown in Fig. 3 using a photolithographic process on a 300 nm-thick YBCO film deposited onto a 1 mm-thick sapphire
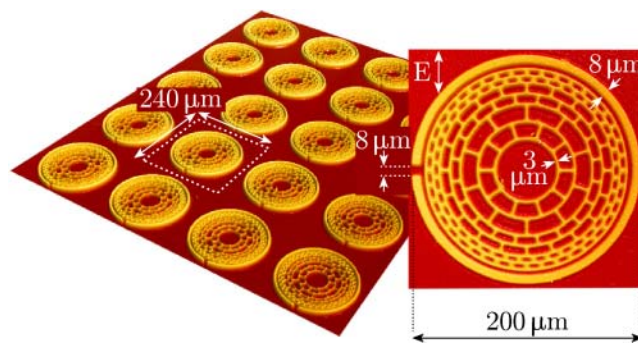

Figure 3 | **Realization of the Woodcut superconducting quantum metamaterial.** The interference microscope picture of a fragment of the woodcut metamaterial (colour expresses height). The metamaterial is created by patterning 300 nm thick YBCO film deposited onto 1 mm thick sapphire substrate and covers an area of 30 mm in diameter.

substrate. The outer and inner radii of the split-ring resonator (SRR) are 100 μm and 92 μm respectively; the gap in the SRR is 8 μm wide. The outer radius of the inner mesh is 89 μm. All the wire-strips inside the inner mesh, were designed to be 3 μm wide, but due to manufacturing uncertainties most notable on the outer edge of the mesh, the wire width is slightly greater. The metamaterial unit cell size is 240 μm × 240 μm. Full 3-dimensional Maxwell calculation show that in this metamaterial structure, at T = 77 K, near the resonant frequency of ~95 GHz, at the incident radiation intensity of ~1 W/cm² the flux switching will be seen: the current through the outer rim of the mesh will reach ~10 mA, i.e. the critical current in YBCO, whilst the amplitude of the magnetic flux applied to each closed loop in the outer rim of the mesh will be of order Φ_0.

Electromagnetic characterization. The level of intensity of ~1 W/cm² required to demonstrate switching was not achievable in our experimental setup and we characterized electromagnetic properties of the woodcut metamaterial in the flux exclusion regime only (Fig. 4). To evaluate the potential switching of electromagnetic properties from the flux exclusion to the flux penetration regimes, we experimentally modeled the two regimes by comparing the measured transmission of the split-ring metamaterial and the metamaterial with split-ring resonators containing the field-blocking nested disks (inside the split rings). These two reference metamaterials represent the two extreme modes of the woodcut metamaterial operation: the flux exclusion and the flux penetration mode.

All three metamaterials shared the same unit cell and split-ring dimensions and were manufactured by the same technological process (see Methods). The free-space electromagnetic response of the three metamaterials in the 75 GHz-110 GHz frequency range was characterized using a network analyzer and focusing horn antennas. The metamaterial samples were placed in a closed-cycle cryostat with electromagnetic radiation incident through transparent windows. The intensity of incident radiation reaching the metamaterials was of the order of 50 μW/cm². The metamaterials demonstrated a clear Lorentzian-like resonant dip in transmission, shifting towards the lower frequencies and becoming shallower as the temperature reached the critical temperature of the superconductor (83 K).

Discussion
Expected change in the woodcut metamaterial's transmission upon flux switching is illustrated in Fig. 4a,b. The Maxwell calculations (Fig. 4a) and the experiment (Fig. 4b) show that flux penetration leads to an up-shift in the resonance frequency of the metamaterial array. The experimentally observed value of the shift is about 7 GHz for temperatures below 60 K, decreasing towards critical temperature of superconductivity. This shift is well replicated by calculations (Fig. 4a,b). Some minor discrepancies between experi-
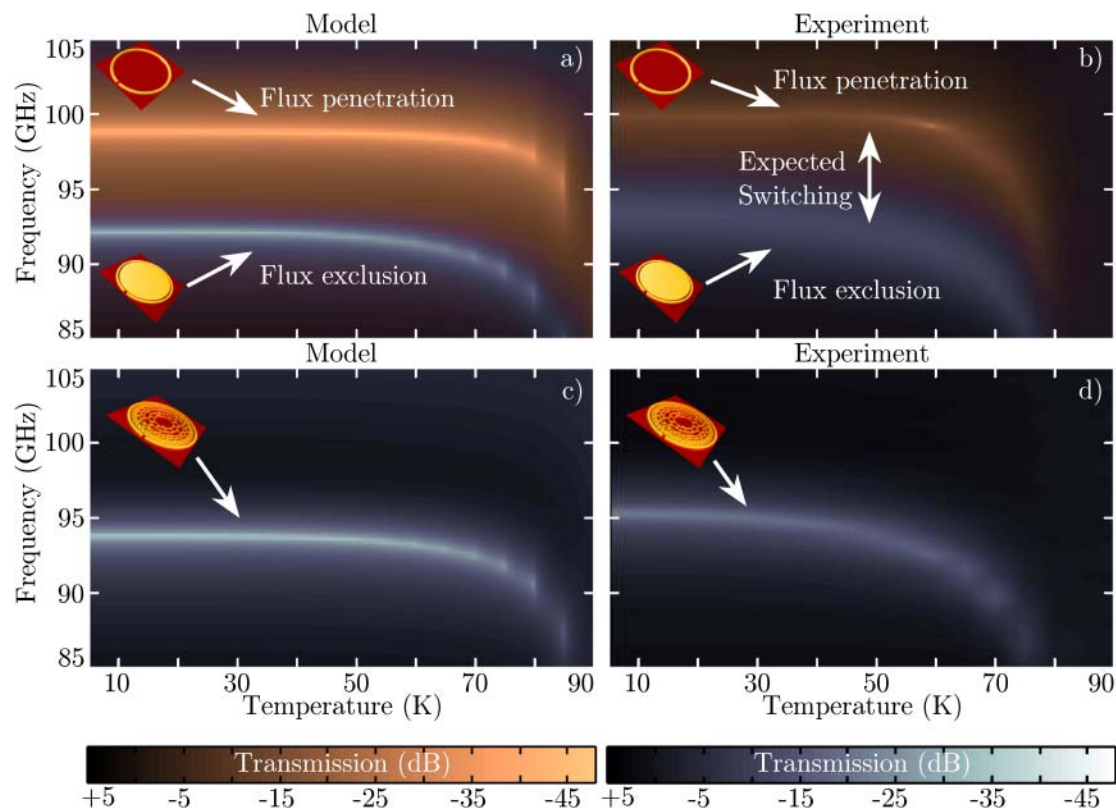
Figure 4 | **Electromagnetic properties of the woodcut metamaterial and reference metamaterial structures.** Computed (a) and experimentally observed (b) transmission spectra of split-ring superconducting metamaterial with and without the nested superconducting disk (yellow and blue respectively) as functions of temperature; Computed (c) and measured (d) transmission of the woodcut flux exclusion quantum metamaterial.

mentally measured and calculated characteristics of the metamaterial response are explainable by tolerance of the fabrication process (widths of lines and gaps in the designs) and simplifications of the two-fluid model of superconductivity that does not account for any anisotropy of the material's response.

We expect that upon reaching the excitation level of ∼1 W/cm² the woodcut metamaterial will exhibit a similar ∼7 GHz shift in transmission resulting in ∼20 dB of transmission change. However, the exact dynamics of this shift which is likely to take the form of a hysteretic nonlinear response, is difficult to predict and it has to be investigated both theoretically and experimentally in the future.

At this stage we should note, that experimentally observed transmission spectra for the woodcut metamaterial (Fig. 4d) are closely matched by the transmission spectrum of the empty split ring metamaterial with field-blocking disk, as would be expected for the flux exclusion regime. We therefore conclude that at intensity level of 50 µW/cm² the woodcut metamaterial remains in the flux exclusion state. As far as we are aware this is the first observation of the quantum phenomenon of flux exclusion affecting the macroscopic properties of a metamaterial. Here one can see a nearly perfect corroboration between the computed (Fig. 4c) and experimentally measured values (Fig. 4d) of woodcut metamaterial transmission. The good agreement between the full 3-dimensional Maxwell calculations and experimental spectra indicates a high quality of the samples and thus a non-destructive nature of the fabrication process (superconducting properties of remaining YBCO are not diminished). This gives us confidence that a quantum-level flux penetration switching will be observable in these structures at the higher intensity levels.

In conclusion, a new type of superconducting metamaterial capable of quantum level nonlinear response underpinned by flux quantization has been designed, modeled, manufactured from a high-temperature superconductor and characterized in low-intensity, flux exclusion regime. Measurements on model metamaterial samples have

demonstrated the extent of the expected change in the metamaterial's transmission upon switching. Quantum metamaterials based on the proposed principle could find applications in active devices for controlling THz and sub-THz radiation.

Methods

Metamaterial fabrication. The metamaterials have been created by patterning the 300 nm-thick YBCO film (critical temperature 83 K, critical current density 10^6 A/cm² at temperature 77 K) on 1 mm-thick sapphire substrate which was deposited by commercial supplier (Theva, Germany). Substrate was a disk of diameter 30 mm. The patterning was carried out using UV-photolithography followed by ion beam milling (dry etching).

Housing of metamaterial. The metamaterials have been placed inside an closed-cycle helium-cooled optical cryostat. The cryostat was equipped with a temperature sensor and an electric resistance heater. This allowed to control the metamaterial temperature within the range T=5 K…300 K.

Transmission data acquisition. The transmission of sub-terahertz radiation has been measured in range 75 – 110 GHz using microwave vector network analyzer (Agilent) with sub-terahertz adapter antennas. The output power of the adapter antennas has been measred with a commercially supplied power meter. The frequency-dependent attenuation of the cryostat has been measured (typically 50% of radiation intensity was lost on the way from antenna to metamaterial) in a separate experiment and used to calculate the exact radiation intensity incident on the metamaterial.

1. Zheludev, N. I. The road ahead for metamaterials. *Science* **328**, 582–583 (2010).
2. Tsiatmas, A., Fedotov, V. A. & Zheludev, N. I. Plasmonics without losses? (the case for terahertz superconducting plasmonics) *arXiv* **1105.3045** (2011).
3. Staffaroni, M., Conway, J., Vedantam, S., Tang, J. & Yablonovitch, E. Circuit analysis in metal-optics. *arXiv* **1006.3126** (2010).
4. Tsiatmas, A. *et al.* Superconducting plasmonics and extraordinary transmission. *Appl. Phys. Lett.* **97**, 111106 (2010).
5. Tian, Z. *et al.* Terahertz superconducting plasmonic hole array. *Opt. Lett.* **35**, 3586–3588 (2010).

6. Kurter, C. *et al.* Classical analogue of electromagnetically induced transparency with a metal-superconductor hybrid metamaterial. *Phys. Rev. Lett.* **107**, 043901 (2011).
7. Wu, J. *et al.* Superconducting terahertz metamaterials mimicking electromagnetically induced transparency. *Appl. Phys. Lett.* **99**, 161113 (2011).
8. Ricci, M., Orloff, N. & Anlage, S. M. Superconducting metamaterials. *Appl. Phys. Lett.* **87**, 034102 (2005).
9. Gu, J. *et al.* Terahertz superconductor metamaterial. *Appl. Phys. Lett.* **97**, 071102 (2010).
10. Wu, J. *et al.* Tuning of superconducting niobium nitride terahertz metamaterials. *Opt. Express* **19**, 12021–12026 (2011).
11. Fedotov, V. A. *et al.* Temperature control of Fano resonances and transmission in superconducting metamaterials. *Opt. Express* **18**, 9015–9019 (2010).
12. Chen, H. *et al.* Tuning the resonance in high-temperature superconducting terahertz metamaterials. *Phys. Rev. Lett.* **105**, 247402 (2010).
13. Jin, B. *et al.* Low loss and magnetic field-tunable superconducting terahertz metamaterial. *Opt. Express* **18**, 17504–17509 (2010).
14. Tsiatmas, A., Buckingham, A. R., Savinov, V., Fedotov, V. A., de Groot, P. A. J. & Zheludev, N. I. Realising tunable, quantum and low-loss metamaterials and plasmonics with superconductors. In *Metamaterials 2011, Barcelona, Spain, 10–15 Oct* (2011).
15. Du, C., Chen, H. & Li, S. Quantum left-handed metamaterial from superconducting quantum-interference devices. *Phys. Rev. B* **74**, 113105 (2006).
16. Lazarides, N. & Tsironis, G. P. rf superconducting quantum interference device metamaterials. *Appl. Phys. Lett.* **90**, 163501 (2007).
17. Du, C., Chen, H. & Li, S. Stable and bistable SQUID metamaterials. *J. Phys.: Condens. Matter* **20**, 345220 (2008).
18. Maimistov, A. I. & Gabitov, I. R. Nonlinear response of a thin metamaterial film containing Josephson junctions. *Opt. Commun.* **283**, 1633–1639 (2010).
19. Rakhmanov, A. L., Zagoskin, A. M., Savel'ev, S. & Nori, F. Quantum metamaterials: Electromagnetic waves in a Josephson qubit line. *Phys. Rev. B* **77**, 144507 (2008).
20. Clarke, J. & Wilhelm, F. K. Superconducting quantum bits. *Nature* **453**, 1031–1042 (2008).
21. You, J. Q. & Nori, F. Atomic physics and quantum optics using superconducting circuits. *Nature* **474**, 589–597 (2011).
22. Castellanos-Beltran, M. A., Irwin, K. D., Hilton, G. C., Vale, L. R. & Lehnert, K. W. Amplification and squeezing of quantum noise with a tunable Josephson metamaterial. *Nature Phys.* **4**, 929–931 (2008).
23. Sadovskii, M. V. High-temperature superconductivity in iron-based compounds. *Phys.-Usp.* **51**, 1201–1227 (2008).
24. van Duzer, T. & Turner, C. W. *Principles of Superconductive Devices and Circuits* (Edward Arnold, 1981).
25. Doettinger, S. G. *et al.* Electronic instability at high flux-flow velocities in high-T$_c$ superconducting films. *Phys. Rev. Lett.* **73**, 1691 (1994).
26. Grimaldi, G. Leo, A., Nigro, A., Pace, S., Cirillo, C. & Attanasio, C. Thickness dependence of vortex critical velocity in wide Nb films. *Physica C* **468**, 765–768 (2008).
27. Jelila, F. S. *et al.* Time of Nucleation of Phase-Slip Centers in YBa$_2$Cu$_3$O$_7$ Superconducting Bridges. *Phys. Rev. Lett.* **81**, 1933 (1998).
28. Sabouret, G., Williams, C. & Sobolewski, R. Resistive switching dynamics in current-biased YBa$_2$Cu$_3$O$_{7-x}$ microbridges excited by nanosecond electrical pulses. *Phys. Rev. B* **66**, 132501 (2002).
29. Pedersen, S., Kofod, G. R., Hollingbery, J. C., Sørensen, C. B. & Lindelof, P. E. Dilation of the giant vortex state in a mesoscopic superconducting loop. *Phys. Rev. B* **64**, 104522 (2001).
30. Silver, A. H. & Zimmerman, J. E. Quantum states and transitions in weakly connected superconducting rings. *Phys. Rev.* **157**, 317–341 (1967).
31. Vendik, O. G., Vendik, I. B. & Kaparkov, D. I. Emperical model of the microwave properties of high-temperature superconductors. *IEEE Trans. Microw. Theory Tech.* **46**, 469–478 (1998).
32. González, M. T., Viña, J., Currás, S. R., Veira, J. A., Maza, J. & Vidal, F. Normal-superconducting transition induced by high current densities in YBa$_2$Cu$_3$O$_{7-\delta}$ melt-textured samples and thin films: Similarities and differences. *Phys. Rev. B* **68**, 054514 (2003).
33. Nuss, M. C., Mankiewich, P. M., O'Malley, M. L., Westerwick, E. H. & Littlewood, P. B. Dynamic Conductivity and "Coherence Peak" in YBa$_2$Cu$_3$O$_7$ Superconductors. *Phys. Rev. Lett.* **66**, 3305–3308 (1991).
34. Gao, F., Kruse, J. W., Platt, C. E., Feng, M. & Klein, M. V. Microwave surface impedance at 10 GHz and quasiparticle scattering in YBa$_2$Cu$_3$O$_7$ films. *Appl. Phys. Lett.* **63**, 2274–2276 (1993).
35. Bonn, D .A. *et al.* Microwave determination of the quasiparticle scattering time in YBa$_2$Cu$_3$O$_{6.95}$. *Phys. Rev. B* **47**, 11314–11328 (1993).

Acknowledgments

Author contributions

The principle of flux exclusion metamaterial was proposed by NIZ, VAF, AT and VS. VS and VAF have designed the metamaterial structures. VS performed numerical analysis and manufactured samples jointly with ARB. Characterization experiments were performed by VS with assistance from ARB, AT and VAF. All co-authors contributed to the analysis and interpretation of results. The manuscript was written by VS and NIZ in consultation with all other co-authors. NIZ supervised the project.

Additional information

How to cite this article: Savinov, V. *et al.* Flux Exclusion Superconducting Quantum Metamaterial: Towards Quantum-level Switching. *Sci. Rep.* **2**, 450; DOI:10.1038/srep00450 (2012).